

# Quantum Yield Measurements of Fluorophores in Lipid Bilayers Using a Plasmonic Nanocavity

Falk Schneider,<sup>†</sup> Daja Ruhlandt,<sup>†</sup> Ingo Gregor, Jörg Enderlein,\* and Alexey I. Chizhik\*<sup>✉</sup>

University of Göttingen, Third Institute of Physics, Friedrich-Hund-Platz 1, 37077 Göttingen, Germany

**ABSTRACT:** Precise knowledge of the quantum yield is important for many fluorescence–spectroscopic techniques, for example, for Förster resonance energy transfer. However, to measure it for emitters in a complex environment and at low concentrations is far from being trivial. Using a plasmonic nanocavity, we measure the absolute quantum yield value of lipid-conjugated dyes incorporated into a supported lipid bilayer. We show that for both hydrophobic and hydrophilic molecules the quantum yield of dyes inside the lipid bilayer strongly differs from its value in aqueous solution. This finding is of particular importance for all fluorescence–spectroscopic studies involving lipid bilayers, such as protein–protein or protein–lipid interactions in membranes or direct fluorescence–spectroscopic measurements of membrane physical properties.



Lipid membranes play key roles in cellular function and viability. They form boundaries for intracellular structures as well as for the cell as a whole and control selective transport of material between cellular compartments or between the exterior and interior of cells. Fluorescence labeling of cell membranes is a standard technique for visualizing them and for watching their temporal evolution and interaction with proteins. For example, membrane staining and visualization allows for monitoring cell shape and volume, adhesion to substrates, as well as membrane organization.<sup>1–4</sup> Besides purely structural imaging, fluorescence spectroscopy can yield even more information about membrane organization, for example, via measurements of FRET between labeled proteins and membrane lipids or between different sorts of membrane lipids. However, a quantitative analysis of fluorescence–spectroscopic data requires knowledge of several key parameters: the excited-state fluorescence lifetime, the orientation of the absorption/emission dipole, excitation and emission spectra, and the fluorescence quantum yield. The latter is defined as the ratio of the number of photons emitted by a fluorophore to the number of photons absorbed.<sup>5–7</sup> In contrast with the other parameters such as lifetime or dipole orientation, the quantum yield of a dye is hard to measure and is either obtained in a comparative manner against a standard or using methods such as the Ulbricht sphere, which is technically challenging and which requires large amounts of sample.<sup>5</sup> This becomes even more challenging if a dye is embedded, at low concentration, within a lipid bilayer of only a few nanometers thickness. The limited sensitivity of most of the quantum yield measurement techniques makes their applicability to such a system impossible.<sup>8</sup> As a result, despite the wide application of fluorescence imaging and spectroscopy to cellular membranes, no quantitative measurement of a fluorophore’s quantum yield in a lipid bilayer has been reported up to now. Hughes et al.

have recently shown that several water-soluble fluorophores strongly change their fluorescence brightness upon interaction with unilamellar lipid vesicles,<sup>9</sup> indicating that it is important to measure the fluorescence properties of membrane-staining dyes when they are associated with a membrane instead of when they are dissolved in solution.

Recently, we have developed a completely new method for absolute quantum yield measurements that is based on the strong electrodynamic interaction of a dye with a metallic nanocavity.<sup>6,10,11</sup> This method has the advantage of being extremely sensitive (requiring only minute amounts of sample) and very versatile (e.g., allowing to measure quantum yields of dyes within thin a lipid bilayer). Using this nanocavity-based quantum yield measurement technique, we present here results of absolute quantum yield measurements of hydrophobic (Atto 647N<sup>9,12</sup>) and hydrophilic (Atto 655<sup>9,12</sup>) dyes in solution and as lipid conjugate incorporated into a supported lipid bilayer (SLB). We show that the quantum yield values of both hydrophobic and hydrophilic molecules inside the SLB strongly differ from those of the free dyes in aqueous solution. The measurement is based solely on the nanocavity-induced modulation of the radiative de-excitation rate of molecules and requires no comparison with fluorescence of a known sample.<sup>6,11</sup>

In terms of the radiative ( $k_{\text{rad}}$ ) and nonradiative rates ( $k_{\text{nr}}$ ) of a fluorophore, its quantum yield ( $\Phi$ ) is given by

$$\Phi = \frac{k_{\text{rad}}}{k_{\text{rad}} + k_{\text{nr}}} = k_{\text{rad}}\tau \quad (1)$$

**Received:** February 21, 2017

**Accepted:** March 15, 2017

**Published:** March 15, 2017

where  $\tau$  is the excited-state lifetime (fluorescence lifetime) of the fluorophore. By modeling the cavity-induced change of the fluorophores' radiative rate  $k_{\text{rad}}$  by an accurate physical model and then fitting the model curve to the measured excited-state lifetime  $\tau$  modulation of the fluorophores inside the cavity, it is possible to determine an absolute value of its quantum yield.

Experimentally, we used a plasmonic nanocavity and a custom-built scanning confocal microscope that is schematically shown in Figure 1. The cavity mirrors were prepared by vapor

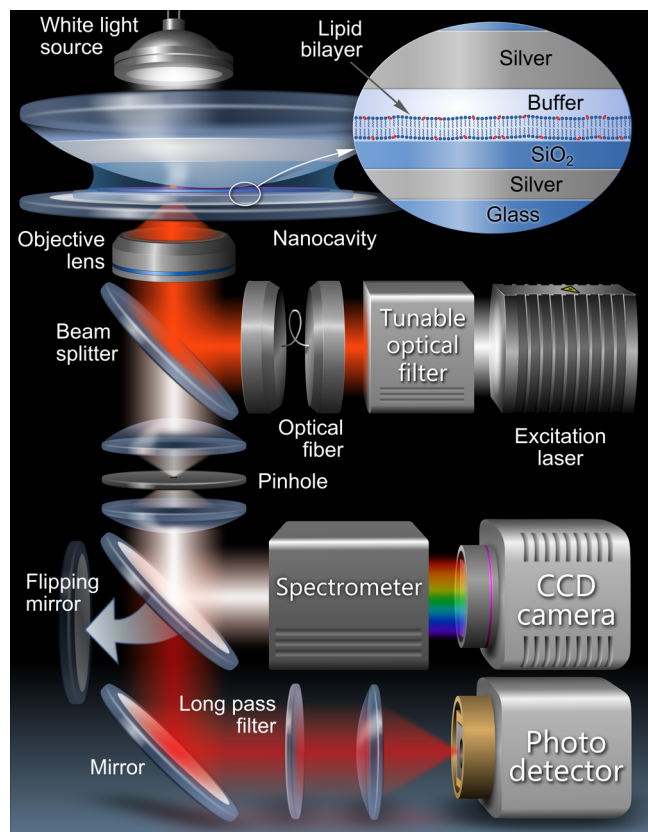


**Figure 1.** Schematic of the confocal scanning microscope and the plasmonic nanocavity that were used for measuring absolute quantum yields of fluorophores inside lipid bilayers. The inset shows the structure of the sample inside the cavity.

deposition of silver on the surface of a clean glass cover slide (bottom mirror) and a plane-convex lens (top mirror) by using a Laybold Univex 350 evaporation machine under high-vacuum conditions ( $\sim 10^{-6}$  mbar). The bottom and top mirrors had a thickness of 30 and 60 nm, respectively. For the measurements of molecules within the SLB, the bottom mirror was additionally coated with a 30 nm thick  $\text{SiO}_2$  layer to decrease direct fluorescence quenching by the metal mirror and to provide a hydrophilic support for the lipid bilayer formation.

The distance between the cavity mirrors was monitored by measuring the white-light transmission spectrum using an Andor SR 303i spectrograph and a CCD camera (Andor iXon DU897 BV). By fitting these spectra with a standard Fresnel model of transmission through a stack of plane-parallel layers, one can determine the precise cavity length (distance between mirrors).

Fluorescence lifetime measurements were performed with a custom-built confocal microscope equipped with an objective lens of high numerical aperture (Apo N, 60 $\times$  /1.49 NA oil immersion, Olympus). A white-light laser system (Fianium SC400-4-20) with a tunable filter (AOTFnC-400.650-TN) served as excitation source ( $\lambda_{\text{exc}} = 640$  nm). Collected fluorescence was focused onto the active area of a single photon detection module (MPD series, PDM). Data acquisition was accomplished with a multichannel picosecond event timer (HydraHarp 400). Photon arrival times were histogrammed (bin width of 50 ps) for obtaining fluorescence decay curves. Finally, the average excited-state lifetime was calculated according to

$$\langle \tau \rangle = \int_0^{\infty} F(t)t dt / \int_0^{\infty} F(t)dt \quad (2)$$

SLBs are commonly used models of cell membranes.<sup>13–15</sup> In our experiments, SLBs were formed by spin-coating a lipid mixture on the surface of the  $\text{SiO}_2$ -coated cavity mirror, as previously described in ref 16. In brief, a solution of 1 mg/mL of DOPC (1,2-dioleoyl-*sn*-glycero-3-phosphocholine, Avanti Polar Lipids) dissolved in a 2:1 mixture of chloroform and methanol was spin-coated using a spin-coater (WS-400-6NPP, Laurell Technologies) at 3000 rpm for 45 s. To incorporate the fluorescent lipid analogues Atto 647N-DOPE and Atto 655-DPPE into the bilayer, they were added to the DOPC solution at ratios between 1:20 000 and 1:50 000 (w/w). The bilayer was hydrated and washed with SLB buffer containing 150 mM

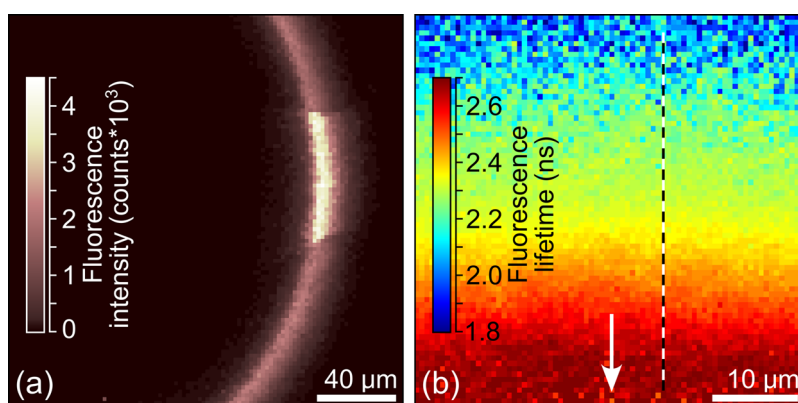


**Figure 2.** Fluorescence confocal scan images of Atto 655 embedded in a lipid bilayer and placed between the cavity mirrors. (a) Fluorescence intensity distribution in the  $\lambda/2$  cavity region. The brightly fluorescent segment of the ring corresponds to an accidentally formed double bilayer. (b) Fluorescence lifetime distribution within the first cavity ring (single bilayer region). The arrow points toward the center of the cavity.

NaCl and 10 mM HEPES. Excess buffer was removed, and the silver-coated lens for the quantum yield measurements was placed on top of the buffer and the SLB. Integrity and fluidity of the bilayers were checked by confocal imaging and fluorescence correlation spectroscopy, respectively. All SLB measurements were performed using lipid-conjugated dyes. The measurements in solution were performed on free dyes Atto 655-NHS and Atto 647N-maleimide, respectively. Atto 647N and Atto 655 dyes were purchased from Atto-Tec (Siegen, Germany).

The concave shape of the upper mirror allows one to easily locate the  $\lambda/2$  region of the cavity, where the cavity-induced modification of the fluorophores' fluorescence lifetime is maximized. Figure 2a shows the measured fluorescence intensity distribution of lipid-conjugated Atto 655 inside the SLB, which is placed between the cavity mirrors. The bright ring segment corresponds to the  $\lambda/2$  region of the cavity, where the emission of the dye is in resonance with the cavity mode. Any off-resonance fluorescence outside the ring is suppressed. The brighter area in the middle of the image, where the signal is about twice as large as in other areas, corresponds to an accidentally formed double bilayer. This, along with the highly homogeneous distribution of fluorescence intensity, proves the integrity and homogeneity of the SLB.

Figure 2b shows the measured fluorescence lifetime distribution of Atto 655 inside the single SLB within the  $\lambda/2$  region of the nanocavity. To determine the dependence of the fluorophores' excited-state lifetime as a function of cavity length, we recorded both the fluorescence decay curve and the cavity white-light transmission spectrum for several points along the dashed line in Figure 2b.

The solid circles in Figure 3a,b show the results of the fluorescence lifetime measurements at different maximum transmission wavelengths (linearly proportional to the cavity length) for Atto 647N and Atto 655 inside the SLB, respectively. The solid curves are theoretical fits to the experimental data, which result in fluorescence quantum yield values of 77% (Atto 647N-DOPE) and 46% (Atto 655-DPPE). The theoretical model takes into account the whole geometry of the cavity as well as the location of the dye-labeled SLB, which allows us to precisely describe the cavity-induced modulation of the fluorophores' radiative rate (see refs 6 and 10 for further details). The second free parameter in our theoretical model is the excited-state lifetime of the fluorophore in the absence of the cavity ( $\tau$  in Figure 3). We use it to verify the validity of our quantum yield measurements by comparing the fitted lifetime values (i.e., extracted from the fit of our theoretical model of lifetime-versus-cavity-length dependence to the experimental data) with those that are directly measured in an SLB deposited on a pure glass cover slide. The discrepancy between the fitted and directly measured lifetime values does not exceed 5%, which indicates the reliability of the obtained quantum yield values.

For measuring the quantum yield of dye molecules in water, we placed a droplet of submicromolar aqueous solution between the silver mirrors without additional SiO<sub>2</sub> coating (identical design to the one reported in refs 6 and 17). As in the previous experiment, the measurements of the fluorescence decay curves at different cavity lengths were done within the  $\lambda/2$  region of the cavity. The measured data for Atto 647N and Atto 655 are shown by open circles in Figure 3a,b, respectively. The dashed curves represent fits of the theoretical model, where the free-fit parameters were again the free-space lifetime  $\tau$  and the fluorescence quantum yield  $\Phi$ . Despite the chemical

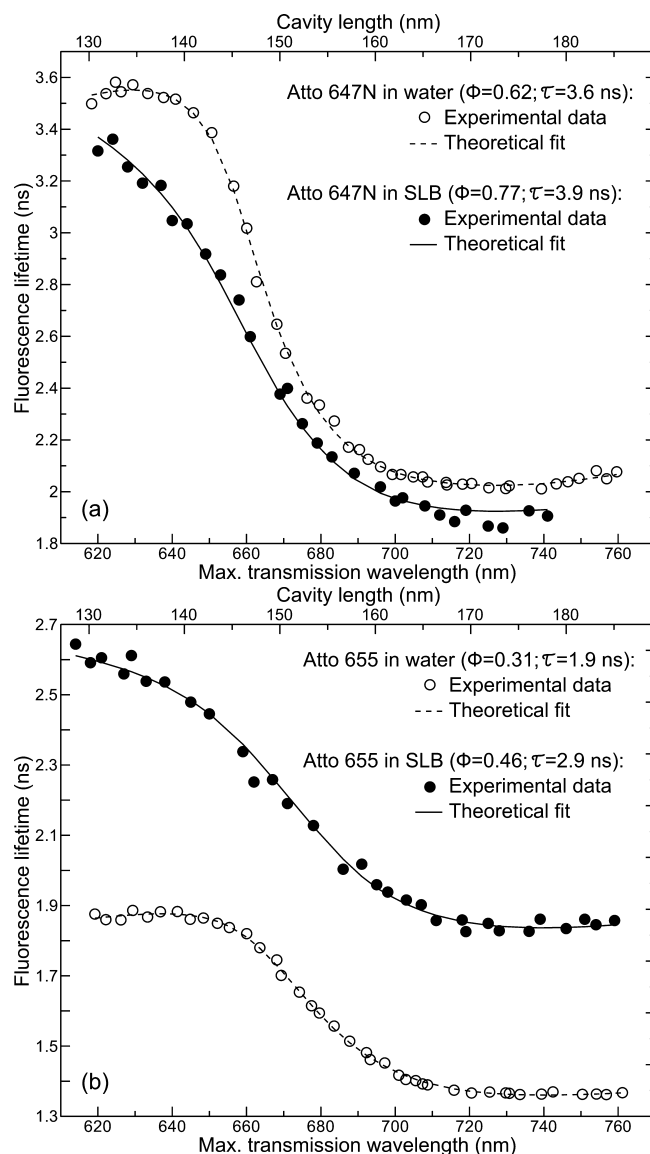


**Figure 3.** Excited-state lifetime of Atto 647N (a) and Atto 655 (b) as a function of the maximum transmission wavelength (linearly proportional to the cavity length) of the nanocavity. Solid and open circles are data that were measured within the supported lipid bilayer and in aqueous solution, respectively. Solid and dashed curves are the fits of the theoretical model to the experimental data. The fit parameters are the fluorescence quantum yield ( $\Phi$ ) and the free lifetime in the absence of the cavity ( $\tau$ ).

identity of the fluorophores in both experiments, the curves show a drastic difference between the cavity-induced fluorescence lifetime modulation for molecules in the SLB and in aqueous solution. Above all, this is caused by the different distribution of molecules within the cavity when measuring in a SLB or in solution.<sup>10</sup> Next (and most important here), it is caused by the different nonradiative de-excitation rates of the dyes in the SLB and in solution, resulting in different quantum yield values. The increase in the quantum yield from 62 to 77% for Atto 647N and from 31 to 46% for Atto 655 when embedding them into the SLB suggests that a drastic change of the photophysical properties of fluorophores in SLBs is a common phenomenon for both hydrophobic and hydrophilic dyes. Most probably, this huge change in quantum yield is due to the strong difference of the polarity of an

aqueous buffer and that of a lipid bilayer, which is known to have a strong impact on fluorescence properties. It should be noted that the change of the quantum yield upon embedding in a lipid membrane will also modify other photophysical properties such as bleaching rate, FRET efficiency, brightness, or interaction with plasmonic nanostructures. This makes our finding important for a large variety of fluorescence-spectroscopic and microscopic techniques.<sup>3,4</sup> Finally, the absolute quantitative characterization of the fluorescence quantum yield is of importance for studies of interactions between membrane proteins and lipid bilayers.<sup>2,18,19</sup>

In summary, we have shown that the fluorescence quantum yield of both hydrophobic and hydrophilic molecules embedded inside a lipid bilayer strongly changes in comparison with the same type of molecules dissolved in an aqueous solution. Using a plasmonic nanocavity, we measured the modulation of the radiative rate of these molecules as a function of cavity length. By comparing theoretically modeled and experimentally measured modulation curves, we could determine absolute values of the dyes' fluorescence quantum yield both in solution and inside a lipid bilayer.

## AUTHOR INFORMATION

### Corresponding Authors

\*E-mail: [jenderl@gwdg.de](mailto:jenderl@gwdg.de) (J.E.).

\*E-mail: [alexey.chizhik@phys.uni-goettingen.de](mailto:alexey.chizhik@phys.uni-goettingen.de) (A.I.C.).

### ORCID

Alexey I. Chizhik: [0000-0003-0454-5924](https://orcid.org/0000-0003-0454-5924)

### Author Contributions

<sup>†</sup>F.S. and D.R. contributed equally to this work.

### Notes

The authors declare no competing financial interest.

## ACKNOWLEDGMENTS

Funding by the German Science Foundation (DFG, SFB 937, project A14) is gratefully acknowledged. We thank Anna Chizhik and Jan Thiart for technical support.

## REFERENCES

- (1) Bagatolli, L. A., *Membranes and Fluorescence Microscopy. In Reviews in Fluorescence 2007*; Springer New York: New York, NY, 2009; pp 33–51.
- (2) Andersen, O. S.; Koeppe, R. E. Bilayer Thickness and Membrane Protein Function: An Energetic Perspective. *Annu. Rev. Biophys. Biomol. Struct.* **2007**, *36*, 107–130.
- (3) Chizhik, A. I.; Rother, J.; Gregor, I.; Janshoff, A.; Enderlein, J. Metal-Induced Energy Transfer for Live Cell Nanoscopy. *Nat. Photonics* **2014**, *8*, 124–127.
- (4) Eggeling, C.; Ringemann, C.; Medda, R.; Schwarzmann, G.; Sandhoff, K.; Polyakova, S.; Below, V. N.; Hein, B.; von Middendorff, C.; Schonle, A.; Hell, S. W. Direct Observation of the Nanoscale Dynamics of Membrane Lipids in a Living Cell. *Nature* **2009**, *457*, 1159–1162.
- (5) Würth, C.; Grabolle, M.; Pauli, J.; Spieles, M.; Resch-Genger, U. Relative and Absolute Determination of Fluorescence Quantum Yields of Transparent Samples. *Nat. Protoc.* **2013**, *8*, 1535–1550.
- (6) Chizhik, A. I.; Gregor, I.; Ernst, B.; Enderlein, J. Nanocavity-Based Determination of Absolute Values of Photoluminescence Quantum Yields. *ChemPhysChem* **2013**, *14*, 505–513.
- (7) Introduction to Fluorescence. In *Principles of Fluorescence Spectroscopy*; Lakowicz, J. R., Ed.; Springer: Boston, 2006; pp 1–26.
- (8) Karedla, N.; Enderlein, J.; Gregor, I.; Chizhik, A. I. Absolute Photoluminescence Quantum Yield Measurement in a Complex

Nanoscope System with Multiple Overlapping States. *J. Phys. Chem. Lett.* **2014**, *5*, 1198–1202.

(9) Hughes, L. D.; Rawle, R. J.; Boxer, S. G. Choose Your Label Wisely: Water-Soluble Fluorophores Often Interact with Lipid Bilayers. *PLoS One* **2014**, *9*, e87649.

(10) Chizhik, A. I.; Gregor, I.; Schleifenbaum, F.; Müller, C. B.; Röling, C.; Meixner, A. J.; Enderlein, J. Electrodynamic Coupling of Electric Dipole Emitters to a Fluctuating Mode Density within a Nanocavity. *Phys. Rev. Lett.* **2012**, *108*, 163002.

(11) Chizhik, A. I.; Chizhik, A. M.; Khoptyar, D.; Bär, S.; Meixner, A. J.; Enderlein, J. Probing the Radiative Transition of Single Molecules with a Tunable Microresonator. *Nano Lett.* **2011**, *11*, 1700–1703.

(12) van de Linde, S.; Krstic, I.; Prisner, T.; Dooze, S.; Heilemann, M.; Sauer, M. Photoinduced Formation of Reversible Dye Radicals and Their Impact on Super-Resolution Imaging. *Photochemical & Photobiological Sciences* **2011**, *10*, 499–506.

(13) Steinem, C.; Janshoff, A.; Ulrich, W.-P.; Sieber, M.; Galla, H.-J. Impedance Analysis of Supported Lipid Bilayer Membranes: a Scrutiny of Different Preparation Techniques. *Biochim. Biophys. Acta, Biomembr.* **1996**, *1279*, 169–180.

(14) Richter, R. P.; Brisson, A. R. Following the Formation of Supported Lipid Bilayers on Mica: A Study Combining AFM, QCM-D, and Ellipsometry. *Biophys. J.* **2005**, *88*, 3422–3433.

(15) Richter, R. P.; Bérat, R.; Brisson, A. R. Formation of Solid-Supported Lipid Bilayers: An Integrated View. *Langmuir* **2006**, *22*, 3497–3505.

(16) Clausen, M. P.; Sezgin, E.; Bernardino de la Serna, J.; Waithe, D.; Lagerholm, B. C.; Eggeling, C. A Straightforward Approach for Gated STED-FCS to Investigate Lipid Membrane Dynamics. *Methods* **2015**, *88*, 67–75.

(17) Chizhik, A. I.; Gregor, I.; Enderlein, J. Quantum Yield Measurement in a Multicolor Chromophore Solution Using a Nanocavity. *Nano Lett.* **2013**, *13*, 1348–1351.

(18) King, C.; Sarabipour, S.; Byrne, P.; Leahy, D. J.; Hristova, K. The FRET Signatures of Noninteracting Proteins in Membranes: Simulations and Experiments. *Biophys. J.* **2014**, *106*, 1309–1317.

(19) Phillips, R.; Ursell, T.; Wiggins, P.; Sens, P. Emerging Roles for Lipids in Shaping Membrane-Protein Function. *Nature* **2009**, *459*, 379–385.